Kinetics and Thermochemistry of the Reactions of CH_3CCl_2 and $(CH_3)_2CCl$ Radicals with Molecular Oxygen

Vadim D. Knyazev,* Ákos Bencsura,† and Irene R. Slagle*

Department of Chemistry, The Catholic University of America, Washington, D.C. 20064

Received: August 11, 1997; In Final Form: November 6, 1997

The kinetics of the reactions $CH_3CCl_2 + O_2 \rightleftharpoons CH_3CCl_2O_2 \rightarrow$ products (1) and $(CH_3)_2CCl + O_2 \rightleftharpoons (CH_3)_2CClO_2 \rightarrow$ products (2) have been studied using laser photolysis/photoionization mass spectrometry. Decay constants of the radicals were determined in time-resolved experiments as a function of temperature (299−1000 K (reaction 1) and 299−700 K (reaction 2)) and bath gas density ([He] = (3−48) × 10^{16} molecules cm^{-3} (reaction 1) and (3−24) × 10^{16} molecules cm^{-3} (reaction 2)). At room temperature the rate constants are in the falloff region under the conditions of the experiments. Relaxation to equilibrium in the addition step of the reaction was monitored within the temperature ranges 430−500 K (reaction 1) and 490−550 K (reaction 2). Equilibrium constants were determined as functions of temperature and used to obtain the enthalpies of the addition step of the reactions 1 and 2. At high temperatures (600−700 K) the rate constant of reaction 2 is independent of both pressure and temperature within the uncertainty of the experimental data and equal to (1.72 ± 0.24) × 10^{-14} cm^3 $molecule^{-1}$ s^{-1}. The rate constant of reaction 1 is independent of pressure within the experimental range and increases with temperature in the high-temperature region: k_1(791 K ≤ T ≤ 1000 K) = (1.74 ± 0.36) × 10^{-12} exp(−6110 ± 179 K/T) cm^3 $molecule^{-1}$ s^{-1}. Structures, vibrational frequencies, and energies of several conformations of $CH_3CCl_2O_2$, $(CH_3)_2CCl$, and $(CH_3)_2CClO_2$ were calculated using ab initio UHF/6-31G** and MP2/6-31G** methods. The results were used to calculate the entropy changes of the addition reactions: $\Delta S°_{298}$ = −159.6 ± 4.0 J mol^{-1} K^{-1} (reaction 1) and $\Delta S°_{298}$ = −165.5 ± 6.0 J mol^{-1} K^{-1} (reaction 2). These entropy changes combined with the experimentally determined equilibrium constants resulted in the R−O_2 bond energies: $\Delta H°_{298}$ = 112.2 ± 2.2 kJ mol^{-1} (reaction 1) and $\Delta H°_{298}$ = 136.0 ± 3.8 kJ mol^{-1} (reaction 2).

I. Introduction

Due to the increasing usage of combustion as a treatment process for the disposal of hazardous organic wastes, including chlorinated hydrocarbons (CHC), kinetic modeling of the combustion of CHCs is a growing field of study. Fundamental knowledge about the mechanisms, specific pathways, and kinetic parameters of important elementary reactions, including the reactions of chlorinated alkyl radicals, are needed for the success of such modeling.

Oxidation of polyatomic free radicals (R) by molecular oxygen is a key elementary step in the combustion processes. The kinetics of the reactions of chlorine-containing alkyl radicals with O_2 has not been extensively studied, especially at high temperatures. The addition process, which is the dominant reaction path at low temperatures, has been characterized for CH_3CHCl and several chlorinated methyl radicals (refs 1−3, and references therein). The results of studies of the temperature dependence of equilibrium in reactions R + $O_2 \rightleftarrows RO_2$ provide information on the R−O_2 bond energy.[3−6] Such studies have supplied the first measures of the thermal stability of these chlorinated RO_2 intermediates. The bond strengths decrease with increasing chlorination, changing from 137 kJ mol^{-1} for the CH_3 + O_2 reaction to 92 kJ mol^{-1} in the case of CCl_3 + O_2. A similar trend has been found in the case of C_2 radicals: the presence of the Cl atom in the $CH_3CHCl-O_2$ adduct reduced the R−O_2 bond energy by 17 kJ mol^{-1} (from 148 kJ mol^{-1} in the case of $C_2H_5-O_2$[6,7] to 131 kJ mol^{-1} for CH_3CHCl[3]). Such a weakening of the R−O_2 bond caused by the chlorination of R is expected to result in a lowering of the characteristic temperatures at which the change of mechanism of the R + O_2 reaction occurs. This change of mechanism (caused by the thermal instability of RO_2 with respect to dissociation to R + O_2) is a transition from a low-temperature addition reaction to a high-temperature regime where equilibrium in the addition step is reversed and rearrangement of adduct becomes a main reaction pathway.

Here we report the results of an experimental investigation of reactions

$$CH_3CCl_2 + O_2 \rightleftarrows \text{products} \quad (1)$$

$$(CH_3)_2CCl + O_2 \rightleftarrows \text{products} \quad (2)$$

over wide intervals of temperatures and pressures. The distinctly different behavior of reactions 1 and 2 in the low-, intermediate-, and high-temperature regions is quantitatively characterized. Equilibrium constants of the addition step in reactions 1 and 2 were measured as functions of temperature. Properties of $CH_3CCl_2O_2$, $(CH_3)_2CCl$, and $(CH_3)_2CClO_2$ were determined in an ab initio study and used to calculate the entropies of these radicals. These calculated entropy values, together with the experimental equilibrium constants, were used to obtain the R−O_2 bond energies.

† Permanent address: Central Research Institute for Chemistry, Hungarian Academy of Sciences, P.O. Box 17, H-1525 Budapest, Hungary.

S1089-5639(97)02608-X CCC: $15.00
Published on Web 02/14/1998

II. Experimental Section

CH_3CCl_2 and $(CH_3)_2CCl$ radicals were produced at elevated temperatures by pulsed laser photolysis, and their decay was subsequently monitored in time-resolved experiments using photoionization mass spectrometry. Details of the experimental apparatus[8] used have been described before and so are only briefly reviewed here.

Pulsed unfocused 248 (or 193) nm radiation (4 Hz) from a Lambda Physik EMG 201MSC excimer laser was directed along the axis of a heatable quartz reactor (1.05 cm i.d., coated with boron oxide[9] or uncoated). Gas flowing through the tube at $\approx$4 m s^{-1} contained the radical precursor (<1.5%), molecular oxygen in varying concentrations, and an inert carrier gas (He) in large excess. The flowing gas was completely replaced between laser pulses.

Gas was sampled through a hole (0.04 cm diameter) in the side of the reactor and formed into a beam by a conical skimmer before the gas entered the vacuum chamber containing the photoionization mass spectrometer. As the gas beam traversed the ion source, a portion was photoionized and mass selected. CH_3CCl_2 and $(CH_3)_2CCl$ radicals were ionized using the light from a chlorine resonance lamp (8.8−8.9 eV). Temporal ion signal profiles were recorded on a multichannel scaler from a short time before each laser pulse up to 25 ms following the pulse. Data from 1000−71000 repetitions of the experiment were accumulated before the data were analyzed.

CH_3CCl_2 radicals were produced by the pulsed, 193 or 248 nm laser photolysis of 1,1,1-trichloroethane

$$CH_3CCl_3 \xrightarrow{h\nu} CH_3CCl_2 + Cl \qquad (3)$$

$$\rightarrow \text{other products}$$

and $(CH_3)_2CCl$ radicals by that of 2,2-dichloropropane

$$CH_3CCl_2CH_3 \xrightarrow{h\nu} (CH_3)_2CCl + Cl \qquad (4)$$

$$\rightarrow \text{other products}$$

Initial conditions (precursor concentration and laser intensity) were selected to provide low radical concentrations ($\leq 10^{11}$ molecules cm^{-3}) such that reactions between radical products had negligible rates compared to those of the reactions of CH_3CCl_2 and $(CH_3)_2CCl$ with molecular oxygen.

The gases used were obtained from Aldrich (1,1,1-trichloroethane, 99.5% and 2,2-dichloropropane, 98%), Matheson (He, >99.995%; O_2, >99.6%), and Air Products (O_2, >99.96%). Precursors and oxygen were purified by vacuum distillation prior to use. Helium was used as provided.

III. Results

In the absence of molecular oxygen, the kinetics of the CH_3CCl_2 and $(CH_3)_2CCl$ radicals was that of an exponential decay with a first-order constant in the range 0.1−121 s^{-1}. This was attributed to the heterogeneous wall reaction:

$$CH_3CCl_2 \rightarrow \text{heterogeneous loss} \qquad (5)$$

or

$$(CH_3)_2CCl \rightarrow \text{heterogeneous loss} \qquad (6)$$

and, at the highest temperatures, to a contribution from the thermal decomposition of the radical.

Both reactions 1 and 2 displayed distinctly different behavior in low- (room temperature), intermediate-, and high-temperature intervals. While it was possible to experimentally determine bimolecular rate constants of the reactions of CH_3CCl_2 and $(CH_3)_2CCl$ radicals with O_2 in the low- and high-temperature regions, both reactions exhibited nonexponential radical decay in the excess of molecular oxygen at intermediate temperatures. The observed decay curves could be fitted to a double-exponential function. This behavior is indicative of an equilibrium of the type $R + O_2 \rightleftarrows RO_2$:

$$CH_3CCl_2 + O_2 \rightleftarrows CH_3CCl_2O_2 \qquad (1a,-1a)$$

$$(CH_3)_2CCl + O_2 \rightleftarrows (CH_3)_2CClO_2 \qquad (2a,-2a)$$

Attempts to detect the products of reactions 1 and 2 were unsuccessful. $CH_3CCl_2O_2$ and $(CH_3)_2CClO_2$ adducts could not be detected, most likely because of the general low sensitivity of the photoionization mass spectrometry method used here for the detection of peroxy radicals (ref 10 and references therein). The expected (see Discussion) high-temperature products of reactions 1 and 2, CH_2CCl_2 and CH_2CClCH_3 (detected using a hydrogen ionizing lamp with energy 10.2 eV), exhibited not an exponential growth but rather a rapid linear growth following the initial photolysis of precursor. This rapid growth was attributed to chain reactions which followed the initial photolysis of precursors (reactions 3 and 4):

$$\underline{CH_3CCl_3 \xrightarrow{h\nu} CH_3CCl_2 + Cl} \qquad \text{(precursor photolysis)} \quad (3)$$

$$Cl + CH_3CCl_3 \rightarrow HCl + CH_2CCl_3 \qquad \text{(chain propagation)}$$

$$CH_2CCl_3 \rightarrow CH_2CCl_2 + Cl \qquad \text{(chain propagation)}$$

and

$$\underline{CH_3CCl_2CH_3 \xrightarrow{h\nu} (CH_3)_2CCl + Cl} \qquad \text{(precursor photolysis)} \quad (4)$$

$$Cl + CH_3CCl_2CH_3 \rightarrow HCl + CH_2CCl_2CH_3 \qquad \text{(chain propagation)}$$

$$CH_2CCl_2CH_3 \rightarrow CH_2CClCH_3 + Cl \qquad \text{(chain propagation)}$$

Rate constants of reactions $Cl + CH_3CCl_3$ and $Cl + (CH_3)_2CCl_2$ at high temperatures are not known. On the basis of the linear extrapolation of the low-temperature data of Tschuikow-Roux et al.[30] for the $Cl + CH_3CCl_3$ reaction and an analogy with the $Cl + CH_3CHCl_2 \rightarrow HCl + CH_2CHCl_2$ reaction,[30] one can estimate the pseudo-first-order rate constants of the above Cl + RH reactions to be in the ranges 28−240 s^{-1} for RH = CH_3CCl_3 and 64−3600 s^{-1} for RH = $(CH_3)_2CCl_2$ for the conditions of our high-temperature experiments. Any curvature in the Arrhenius dependencies will result in higher values. Thus, it is likely that these chain reactions account for the observed rapid growth of CH_2CCl_2 and CH_2CClCH_3. The possible formation of CH_2CCl_2 and CH_2CClCH_3 in reactions 1 and 2 was effectively obscured by the above chain processes and, therefore, could not be detected.

III.1. Room-Temperature Reaction. At room temperature the decay of CH_3CCl_2 and $(CH_3)_2CCl$ radicals in an excess of O_2 was exponential. The experiments were conducted under pseudo-first-order conditions with $[O_2]$ in the ranges (1.2−19.1)

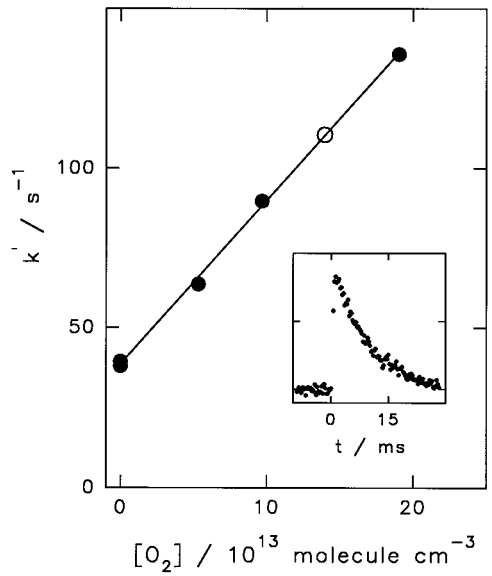

Figure 1. First-order CH_3CCl_2 decay rate k' vs $[O_2]$. The intercept at $[O_2] = 0$ corresponds to the rate of heterogeneous decay of CH_3CCl_2 radicals. $T = 299$ K, $[M] = 6.0 \times 10^{16}$ molecules cm^{-3}, $[CH_3CCl_3] = 6.92 \times 10^{12}$ molecules cm^{-3}. The insert shows the recorded CH_3CCl_2 decay profile for the conditions of the open plotted point: $[O_2] = 1.40 \times 10^{14}$ molecules cm^{-3}, $k' = 110.5 \times b1 \times b1 \pm 2.3$ s^{-1}.

$\times 10^{13}$ molecules cm^{-3} (reaction 1) and $(3.7-20.6) \times 10^{12}$ molecules cm^{-3} (reaction 2). The radical signal profiles were fit to an exponential function ($[R]_t = [R]_0 \exp(-k't)$) by using a nonlinear least-squares procedure. The pseudo-first-order radical decay constants, k', were obtained as a function of the concentration of molecular oxygen. The values of the second-order rate constants, k_1 and k_2, were determined from the slopes of the linear plots of k' vs $[O_2]$ (Figure 1). Experiments were performed to establish that decay constants did not depend on the initial radical concentrations (provided that the concentration was kept low enough to ensure that radical−radical reactions had negligible rates compared to the reaction with O_2), radical precursor concentration, or photolyzing laser intensity. The room-temperature rate constants of reaction 1 were determined at $[He] = (3-48) \times 10^{16}$ atoms cm^{-3} and those of reaction 2 at $[He] = (3-24) \times 10^{16}$ atoms cm^{-3}. The conditions and results of these experiments are presented in Tables 1 and 2. The k' vs $[O_2]$ dependencies for all experiments listed in Tables 1 and 2 are presented in Figures 1S−4S (Supporting Information).

The room-temperature bimolecular rate constants of the reactions of CH_3CCl_2 and $(CH_3)_2CCl$ radicals with molecular oxygen (interpreted as addition reactions 1a and 2a) exhibit a pronounced falloff behavior. The values of k_1 and k_2 increase with pressure within the experimental pressure range (Figure 2). The shapes of these pressure dependencies of k_1 and k_2 are similar to those of the rate constants of the reactions of alkyl (n-C_3H_7)[11] and chlorinated alkyl (CH_3CHCl)[3] radicals of similar size with O_2. The values of k_2 are, on average, an order of magnitude higher than those of k_1 determined at the same densities of the bath gas. This can be explained by the fact that reaction 2 appears to be closer to the high-pressure limit than reaction 1, as expected due to the larger number of vibrational modes in the $(CH_3)_2CClO_2$ adduct.

III.2. High-Temperature Reaction. In the high-temperature region (791−1000 K for reaction 1 and 600−700 K for reaction 2), the decay of CH_3CCl_2 and $(CH_3)_2CCl$ radicals in an excess of O_2 was exponential, as in the case of the room-temperature reaction. The values of the bimolecular rate constants (obtained experimentally by the procedure described above) were lower than the values of k_1 and k_2 obtained at room temperature by 2−3 orders of magnitude. Measuring such low values of rate constants required using high concentrations of O_2 (up to 1.0×10^{17} molecules cm^{-3}). For a set of experiments at a given temperature when high concentrations of O_2 were used, the [He] was reduced accordingly so that the total density of gas ([M]) in the reactor remained constant.

Reaction 1. The rate constants of reaction 1, $CH_3CCl_2 + O_2$, were determined at $T = 791-1000$ K and $[He] = (6-12) \times 10^{16}$ atoms cm^{-3}. The upper temperature limit of the experiments was determined by the onset of thermal decomposition of 1,1-dichloroethyl radicals. At these temperatures CH_3CCl_2 radicals were produced by the lower energy 248 nm photolysis in order to avoid potential high-temperature photolysis or excitation of O_2. The conditions and results of these experiments are presented in Table 1. The values of k_1 obtained were independent of the initial concentration of CH_3CCl_2, laser intensity, radical precursor concentration, and absence or presence of the boron oxide wall coating. To eliminate a possible influence of a minor impurity in oxygen on the measured rate constants, several experiments on reaction 1 were performed using ultrapure carrier grade O_2 (99.96%) obtained from Air Products. No effect of the nominal purity of the oxygen used on the values of k_1 could be detected.

The rate constants of reaction 1 show no dependence on pressure within the experimental range and increase with temperature (Figure 3). The experimental k_1 vs T dependence can be reproduced by an Arrhenius expression:

$$k_1\ (791\ \text{K} \le T \le 1000\ \text{K}) = (1.74 \pm 0.36) \times 10^{-12} \times \exp(-6110 \pm 179\ \text{K}/T)\ \text{cm}^3\ \text{molecule}^{-1}\ \text{s}^{-1} \quad \text{(I)}$$

(Error limits here and throughout the text are 1σ unless otherwise noted.)

Reaction 2. The rate constants of reaction 2, $(CH_3)_2CCl + O_2$, were determined at two temperatures, 600 and 700 K, and two bath gas densities, 6×10^{16} and 12×10^{16} molecules cm^{-3}. The upper temperature limit of the experiments was determined by the rapid increase with temperature of the ion signal background (attributed to a radical precursor ion fragmentation). The conditions and results of these experiments are presented in Table 2. The values of k_2 obtained were independent of the initial radical concentration and the concentration of the radical precursor. Both 193 and 248 nm laser radiation was used to produce $(CH_3)_2CCl$ radicals by the photolysis of $(CH_3)_2CCl_2$, reaction 4. In the experiments where the 248 radiation was used, the obtained rate constants did not depend on the photolyzing laser intensity. When the more energetic 193 nm radiation was used, the slopes of k' vs $[O_2]$ plots exhibited dependence on the laser intensity (L). The apparent values of k_2 decreased with the decreasing laser intensity from $k_2 = 2.65 \times 10^{-14}$ cm^3 molecule^{-1} s^{-1} at $L = 10$ mJ pulse^{-1} cm^{-2} to $k_2 = 2.08 \times 10^{-14}$ cm^3 molecule^{-1} s^{-1} at $L = 6.3$ mJ pulse^{-1} cm^{-2} and to an average value of $\langle k_2 \rangle = 1.73 \times 10^{-14}$ cm^3 molecule^{-1} s^{-1} at L below 4 mJ pulse^{-1} cm^{-2}, where k_2 was independent of L (Table 2). The values of k_2 obtained at low 193 nm laser intensity coincide with the values determined in experiments where the 248 nm photolysis of $(CH_3)_2CCl_2$ was used. We attribute this effect of the apparent k_2 vs L dependence at high L to a contribution from a reaction of $(CH_3)_2CCl$ with the products of the photodissociation or electronic excitation of O_2[12] by the 193 nm radiation at elevated temperatures.

The rate constants of reaction 2 appear to be independent of temperature and pressure within the experimental ranges (Table

TABLE 1: Conditions and Results of Experiments To Measure $k_1(T,[M])^e$

T (K)	$[M]/10^{16}$	$[CH_3CCl_3]/10^{13}$	L^a	$[O_2]/10^{13}$	$k_1/10^{-13}$ (cm^3 $molecule^{-1}$ s^{-1})	k_5 (s^{-1})
299	3.0	1.45	5.0	3.5−15.0	3.21 ± 0.27	33.0
299	6.0	0.69	10.0	5.3−19.1	5.12 ± 1.08	38.7
298	12.0	1.45	1.2	1.3−9.4	8.96 ± 0.99	23.4
298	12.0	1.45	2.9	1.3−9.4	9.16 ± 0.73	29.2
296	24.0	0.67	4.6	2.9−10.9	15.38 ± 1.67	69.1
298	48.0	0.64	2.4	1.2−4.3	20.16 ± 3.04	63.7
791	12.1[b]	17.6	56	(2.1−10.0) × 10^3 [c]	(7.65 ± 0.80) × 10^{-3}	11.2
791	12.1[b]	17.6	22	(2.1−10.0) × 10^3 [c]	(7.77 ± 0.96) × 10^{-3}	7.6
800	12.0[b]	2.2	54	(3.1−7.5) × 10^3	(8.08 ± 0.58) × 10^{-3}	0.1
900	12.0[b]	9.3	13.3	(1.0−6.3) × 10^3	(1.97 ± 0.18) × 10^{-2}	12.2
900	6.0[b]	1.7	52	(0.51−3.43) × 10^3	(2.13 ± 0.29) × 10^{-2}	18.8
938	12.1[b]	7.2	52	(0.88−5.54) × 10^3 [c]	(2.61 ± 0.19) × 10^{-2}	45.3[d]
1000	6.0[b]	5.4	52	(0.78−3.64) × 10^3	(3.62 ± 0.40) × 10^{-2}	121.4[d]

[a] Photolyzing laser intensity (mJ cm^{-2} $pulse^{-1}$). [b] 248 nm photolysis was used (193 nm photolysis was used in all other experiments). [c] Uncoated quartz reactor and ultrapure carrier grade (>99.96%) O_2 were used (quartz reactor coated with boron oxide and lower grade (>99.6%) O_2 were used in all other experiments). [d] Includes contribution from thermal decomposition. [e] Concentrations are in molecules cm^{-3}.

TABLE 2: Conditions and Results of Experiments To Measure $k_2(T,[M])^e$

T (K)	$[M]/10^{16}$	$[(CH_3)_2CCl_2]/10^{13}$	L^a	$[O_2]/10^{13}$	$k_2/10^{-13}$ (cm^3 $molecule^{-1}$ s^{-1})	k_6 (s^{-1})
300	3.0	0.62	6.3	0.69−2.04	51.5 ± 4.2	85.1
299	12.0	0.59	5.4	0.37−1.62	81.3 ± 11.9	57.3
300	12.0	2.65	1.1	0.38−1.49	81.7 ± 6.1	45.7
300	24.0	0.59	5.4	1.05−2.06	85.2 ± 10.1	65.2
600	6.0	158[b]	31	190−648	0.170 ± 0.021	4.2
600	12.0	48.2[b]	59	163−527	0.161 ± 0.018	2.1
700	12.0	59.0[b]	71	203−605	0.173 ± 0.034	16.1
700	12.0	59[b]	30	203−605	0.183 ± 0.025	8.4
700	12.0	2.02	10	191−530	0.265 ± 0.027[c]	23.8
700	12.0	5.94	6.3	320−571	0.208 ± 0.021[c]	18.7
700	12.0	5.94	3.9	320−571	0.169 ± 0.018[c,d]	12.3
700	12.0	8.54	2.9	299−561	0.174 ± 0.020[c,d]	17.0
700	12.0	46.4	0.72	144−556	0.176 ± 0.019[c,d]	30.4

[a] Photolyzing laser intensity (mJ cm^{-2} $pulse^{-1}$). [b] 248 nm photolysis was used (193 nm photolysis was used in all other experiments). [c] The slopes of k′ vs $[O_2]$ plots exhibited dependence on the photolyzing laser intensity (see text). [d] An average of the values of k_2 determined in these three experiments is shown as one point in Figure 3. [e] Concentrations are in molecules cm^{-3}.

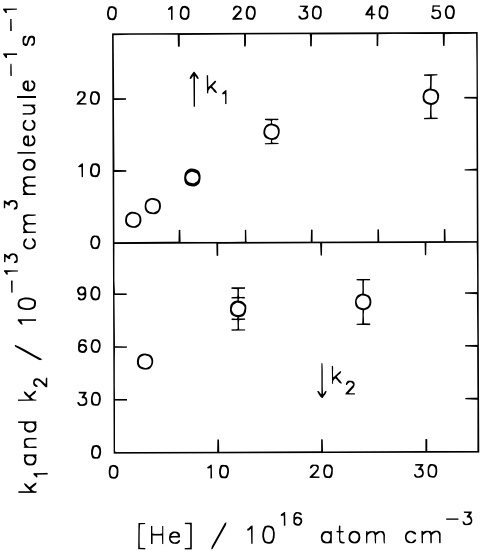

Figure 2. Falloff in the bimolecular rate constants k_1 (upper plot) and k_2 (lower plot) at room temperature.

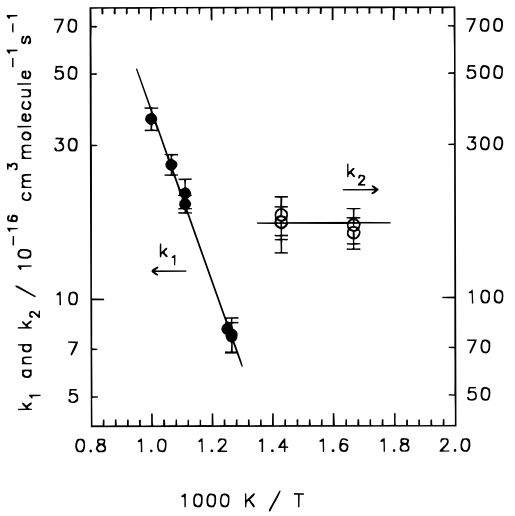

Figure 3. Temperature dependencies of k_1 (filled circles) and k_2 (open circles) in the high-temperature regions. Lines represent Arrhenius fit for $k_1(T)$ (formula I) and an average value of $k_2(T)$.

2). While the experimental temperature interval is too narrow to accurately determine the temperature dependence, the values of k_2 obtained at 600 and 700 K are equal within experimental uncertainties. The average value of k_2 in the high-temperature region is $k_2(600\ K \le T \le 700\ K) = (1.72 \pm 0.24) \times 10^{-14}$ cm^3 $molecule^{-1}$ s^{-1} (Figure 3).

III.3. Intermediate Temperature Ranges. Determination of Equilibrium Constants. In the intermediate temperature ranges (430−500 K for reaction 1 and 490−550 K for reaction 2) the decay of CH_3CCl_2 and $(CH_3)_2CCl$ radicals in the presence of O_2 display a nonexponential behavior, which can be fit with a double-exponential function. In the experiments on reaction 1, the kinetics of CH_3CCl_2 decay was analyzed under the

TABLE 3: Conditions and Results of Experiments To Measure the Equilibrium Constants of Reaction (1,−1)[e]

T/K	[He]/10^{16}	[CH_3CCl_3]/10^{13}	L[a]	[O_2]/10^{15}	k_5/s^{-1}	k_{1a}[O_2]/s^{-1}	k_{-1a}/s^{-1}	k_d/s^{-1}	ln(K_p)[b]	$-f$[c]
430	24.0	1.26	4.2	1.33	9.8	306.7	20.3	4.0	12.167 ± 0.059	0.024
430	24.0	1.26	10	1.33	18.8	308.1	20.2	11.3	12.174 ± 0.061	0.024
440	24.0	1.33	4.2	1.33	8.8	258.2	36.2	8.4	11.390 ± 0.077	0.028
440	12.0	1.09	10	1.19	17.6	148.0	23.7	2.0	11.364 ± 0.092	0.028
450	12.0	1.09	10	1.21	16.8	129.8	45.3	11.3	10.571 ± 0.063	0.032
450	12.0	2.62	2.6	1.83	10.9	185.0	41.3	−0.5	10.584 ± 0.050	0.032
460	6.0	1.06	12	1.32	14.1	90.4	51.7	18.6	9.945 ± 0.089	0.038
460	12.0	1.12	11	0.61	17.1	69.6	83.5	12.2	9.975 ± 0.073	0.038
460	12.0	2.62	2.6	2.38	8.6	305.6	83.8	16.8	10.091 ± 0.062	0.038
470	12.0	1.12	11	0.92	18.2	83.1	83.4	2.5	9.737 ± 0.032	0.044
480	12.0	1.03	13	4.07	21.2	281.5	147.9	22.8	8.862 ± 0.072	0.049
480	12.0	1.03	13	1.90	22.3	172.8	149.9	23.8	9.122 ± 0.066	0.049
480	12.0	1.12	11	0.95	18.4	77.5	126.5	10.4	9.180 ± 0.032	0.049
480	12.0	53.7[d]	54	1.86	2.6	214.7	202.6	0.6	9.061 ± 0.056	0.049
490	12.0	1.03	10	3.41	33.7	172.9	117.1	54.8	8.764 ± 0.046	0.054
490	12.0	1.03	4.2	3.41	31.2	200.1	134.3	54.2	8.773 ± 0.072	0.054
500	6.0	1.06	12	5.89	15.4	221.9	183.1	8.0	8.000 ± 0.098	0.059

[a] Photolyzing laser intensity (mJ cm^{-2} $pulse^{-1}$). [b] Units of K_p are bar^{-1}. Error limits shown here are the values of relative uncertainty ϵ in the K_1 values (see text). [c] Values of the "correction" function (see text, section IV.2). [d] 248 nm photolysis was used (193 nm photolysis was used in all other experiments). [e] Concentrations are in molecules cm^{-3}.

assumption that the following processes are important under these conditions: (1) heterogeneous loss of CH_3CCl_2, reaction 5; (2) reversible addition of O_2, reaction (1a,−1a); (3) decay of the adduct, $CH_3CCl_2O_2$, due to heterogeneous loss and further reaction, which is described by a first-order rate constant k_d. The kinetics of the CH_3CCl_2 radical signal, $I(t)$, in such a system can be described by the following double-exponential expression:[3]

$$I(t) = I_1 \exp(-\lambda_1 t) + I_2 \exp(-\lambda_2 t) \qquad \text{(II)}$$

where

$$I_1 = I_0 \frac{k_{1a}[O_2] + k_5 - \lambda_2}{\lambda_1 - \lambda_2}$$

$$I_2 = I_0 - I_1$$

$$\lambda_{1,2} = \frac{1}{2}(A \pm [A^2 - 4(k_{-1a}k_5 + k_{1a}[O_2]k_d + k_5 k_d)]^{1/2})$$

$$A = k_{1a}[O_2] + k_{-1a} + k_5 + k_d$$

For reaction 2, under identical assumptions, the kinetics of $(CH_3)_2CCl$ is described by the same formulas with k_{1a}, k_{-1a}, and k_5 substituted with k_{2a}, k_{-2a}, and k_6, respectively.

The values of k_5 and k_6 were measured directly in the absence of O_2. The temporal profile of the CH_3CCl_2 signal was fitted to formula II using k_{1a}, K_1, I_0, and k_d as adjustable parameters (here $K_1 = k_{1a}/k_{-1a}$ is the equilibrium constant of the reaction (1a,−1a), and I_0 is the signal value at $t = 0$). After the values of the above parameters were found, the fitting procedure was repeated several times with K_1 fixed at selected values in the vicinity of the best value, and the other three parameters floated. As a result the sum of squares of deviation

$$S = \sum w_i (I_i(t) - I_{calc}(t))^2$$

(weights w_i are inversely proportional to the *signal + background = number of counts per channel* for each $I_i(t)$ point) was determined as a function of K_1 (with the three other parameters optimized) in the vicinity of its minimum and fitted with a parabolic function. From that information the experimental relative uncertainty ϵ of the fitted values of K_1 was determined using standard procedures:[13]

$$\epsilon^2 = \frac{1}{(N-5)} \frac{2}{d^2S/d\xi^2}$$

where N is the number of data points, ξ is a ratio of floated to optimized values of K_1, and S is normalized to be equal to 1 at its minimum. In each experiment to determine the values of K_1 the data were accumulated until the criterion of $\epsilon \leq 10\%$ was satisfied. The equilibrium constants of reaction (1a,−1a) were determined as a function of temperature from 430 to 500 K. The conditions and results of these experiments are presented in Table 3.

The values of the equilibrium constant, K_2, for the reaction (2a,−2a) were determined in a similar procedure at temperatures in the interval 490−550 K. Due to a poorer sensitivity of the experimental apparatus to the detection of the $(CH_3)_2CCl$ (compared to CH_3CCl_2), the experimental constraint on ϵ had to be relaxed to $\epsilon \leq 20\%$. The conditions and results of these experiments are presented in Table 4. Figures 4 and 5 present examples of double-exponential $I(t)$ dependencies for reactions 1 and 2 and corresponding S vs ξ dependencies obtained in the fitting process.

One should note that the conditions of the experiments were selected to optimize only the determination of the equilibrium constants. This results in expected high uncertainties of the $k_{1a}[O_2]$, k_{-1a}, $k_{2a}[O_2]$, k_{-2a}, and k_d kinetic parameters listed in Tables 3 and 4, uncertainties that, in addition, are not easily estimated. The values of k_{1a}, k_{-1a}, k_{2a}, and k_{-2a} are expected to be in the falloff region which will complicate any potential use of these data. Their temperature dependencies exhibit an anticipated qualitative behavior: k_{-1a} and k_{-2a} values increase steeply with temperature (as expected for a rate constant of a decomposition reaction) and the values of k_{1a} and k_{2a} (corresponding to the second-order addition rate constant) somewhat decrease with temperature (as expected for a barrierless addition in the falloff region). The rate constant of the decay of the adduct, k_d, as mentioned above, is a sum of the rate constant of RO_2 heterogeneous loss and that of its possible further reaction to products other than R + O_2. The fitted values of k_d for reactions 1 and 2 lie within the range −8.6 to 55 s^{-1}. Slightly negative values obtained for three points in the fitting process are, certainly, not meaningful and indicate that k_d is close to zero. These low values of k_d indicate that for R = CH_3CCl_2

TABLE 4: Conditions and Results of Experiments To Measure the Equilibrium Constants of Reaction (2,−2)[d]

T/K	[He]/10^{16}	[$(CH_3)_2CCl_2$]/10^{13}	L[a]	[O_2]/10^{14}	k_6/s^{-1}	k_{2a}[O_2]/s^{-1}	k_{-2a}/s^{-1}	k_d/s^{-1}	ln(K_p)[b]	$-f$[c]
490	12.0	1.21	10	3.15	16.1	316.0	25.2	18.1	13.285 ± 0.160	0.062
500	12.0	1.65	10	3.00	14.3	225.0	36.0	−8.6	12.619 ± 0.060	0.068
500	12.0	3.88	1.6	1.45	7.9	198.1	71.2	9.2	12.532 ± 0.051	0.068
510	12.0	1.56	8	1.60	13.2	123.4	47.7	−4.6	12.344 ± 0.134	0.075
520	12.0	1.51	8	1.73	14.2	128.4	94.8	12.5	11.602 ± 0.085	0.083
520	12.0	3.73	3.8	3.82	14.5	217.5	93.1	4.6	11.355 ± 0.051	0.083
520	12.0	3.82	1.6	2.42	8.6	227.8	134.5	8.6	11.489 ± 0.066	0.083
530	12.0	1.37	7	2.14	11.9	174.1	139.4	15.8	11.286 ± 0.100	0.092
540	12.0	1.59	9	4.07	19.5	269.3	178.0	27.2	10.817 ± 0.092	0.100
540	6.0	1.60	9	4.15	17.0	179.0	112.8	7.5	10.846 ± 0.097	0.100
550	6.0	1.65	10	6.70	17.9	315.6	211.8	29.7	10.285 ± 0.140	0.110

[a] Photolyzing laser intensity (mJ cm^{-2} pulse^{-1}). [b] Units of K_p are bar^{-1}. Error limits shown here are the values of relative uncertainty ϵ in the K_2 values (see text). [c] Values of the "correction" function (see text, section IV.2). [d] Concentrations are in molecules cm^{-3}.

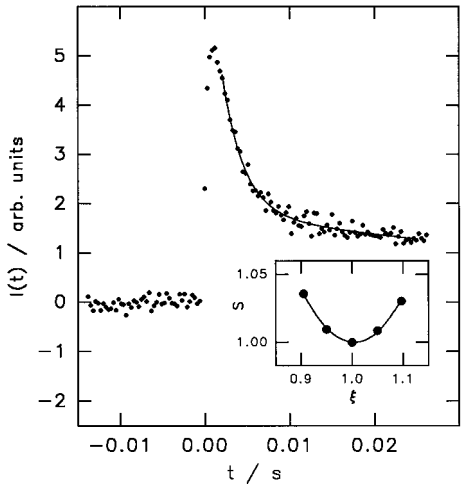

Figure 4. CH_3CCl_2 double-exponential decay profile. $T = 460$ K, [O_2] $= 2.38 \times 10^{15}$ molecules cm^{-3}. The insert shows the normalized sum of squares of deviation, S, vs ξ, the ratio of floated to optimum values of K_1 (see text).

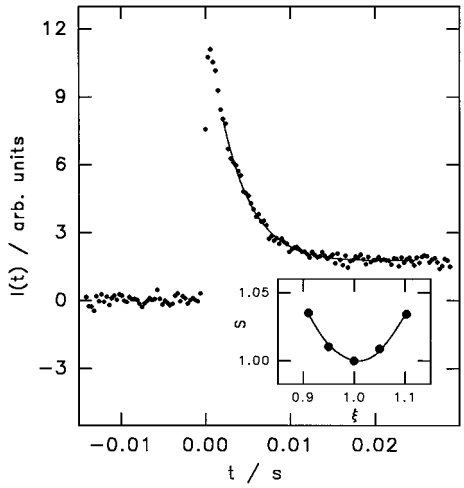

Figure 5. $(CH_3)_2CCl$ double-exponential decay profile. $T = 500$ K, [O_2] $= 3.00 \times 10^{14}$ molecules cm^{-3}. The insert shows the normalized sum of squares of deviation, S, vs ξ, the ratio of floated to optimum values of K_2 (see text).

and $(CH_3)_2CCl$ further reactions of RO_2 (such as isomerization) are minor compared to the reverse decomposition to R + O_2 and the heterogeneous loss of RO_2, most likely, provides the main contribution to k_d.

IV. Thermochemistry of Reactions 1a,−1a and 2a,−2a

The enthalpy changes of reactions (1a,−1a) and (2a,−2a) at room temperature were obtained from the values of $K_1(T)$ and $K_2(T)$ using the third-law analysis. The procedures used have been described before.[3,8,10,14] These calculations require knowledge of the temperature dependencies of the thermodynamic functions (entropy and enthalpy) of the reactants and products of reactions (1a,−1a) and (2a,−2a) which were obtained using the results of ab initio calculations.

IV.1. Molecular Parameters of CH_3CCl_2, $CH_3CCl_2O_2$, $(CH_3)_2CCl$, and $(CH_3)_2ClO_2$. Of all four radicals involved in reactions (1a,−1a) and (2a,−2a), only the properties of CH_3CCl_2 have been studied before. Chen and Tschuikow-Roux[15] optimized geometry and calculated harmonic frequencies at the UHF/6-31G* level of theory and calculated the barrier height for the CH_3 internal rotation at the MP2/6-311G** level. This barrier was found to be equal to 10.3 kJ mol^{-1}, but it slightly reduced to 9.8 kJ mol^{-1} if zero-point vibrational energy was included. We used the latter value together with the rotational constants and vibrational frequencies reported by these authors in our model. Seetula[16] obtained the values of the room-temperature heat of formation and entropy of CH_3CCl_2 from a second-law treatment of the experimental kinetic data on direct (Seetula,[16] $T = 457-787$ K) and reverse (Dymov and Tschuikow-Roux,[17] $T = 308-368$ K) reactions in the CH_3CCl_2 + HBr $\rightleftarrows$ Br + CH_3CHCl_2 system. The entropy of the CH_3CCl_2 radical reported by Seetula, $S°_{298}(CH_3CCl_2) = 288 \pm 5$ J mol^{-1} K^{-1}, is in gross disagreement with the value of 314.7 J mol^{-1} K^{-1} obtained if the CH_3CCl_2 model based on the ab initio study of Chen and Tschuikow-Roux is used. Such a low value of entropy is not consistent with any reasonable model of the CH_3CCl_2 radical. $S°_{298}(CH_3CCl_2)$ can be brought within the error limits reported by Seetula, for example, by assuming a planar structure for the $-CCl_2$ group and increasing the internal rotation barrier and three lowest vibrational frequencies by a factor of 2, which yields $S°_{298}(CH_3CCl_2) = 293$ J mol^{-1} K^{-1}. Such changes of the radical properties, however, are unrealistic.

We studied the geometries and harmonic vibrational frequencies of $CH_3CCl_2O_2$, $(CH_3)_2CCl$, and $(CH_3)_2CClO_2$ using the ab initio unrestricted HF method with 6-31G** basis. Internal rotations ($-CH_3$ torsions and rotation about the C−O bond) were studied by the MP2/6-31G**//UHF/6-31G** method. Geometrical structures corresponding to minima and maxima of the rotational potential energy surfaces were obtained with the full optimization at the UHF/6-31G** level and energy was calculated at the MP2/6-31G** level. Structures, vibrational frequencies, and energies of these species are listed in Tables 1S−5S (Supporting Information). The GAUSSIAN 92 system of programs[18] was used in all ab initio calculations.

The most uncertain aspect of the properties of the radicals pertinent to the calculation of their entropy are the treatments of the hindered internal rotations ($-CH_3$ torsions and rotation about the C−O bond). In all three radicals, $-CH_3$ torsions

TABLE 5: Models of the Molecules Used in the Data Analysis

Vibrational Frequencies (cm^{-1})

CH_3CCl_2:[15]	2979, 2950, 2882, 1459, 1455, 1405, 1100, 1098, 1015, 796, 550, 308, 299, 282
$CH_3CCl_2O_2$:	218, 287, 290, 350, 388, 550, 575, 741, 906, 1083, 1084, 1128, 1142, 1387, 1430, 1433, 2869, 2946, 2960
$(CH_3)_2CCl$:	272, 317, 327, 583, 874, 924, 945, 1034, 1142, 1197, 1371, 1383, 1421, 1429, 1432, 1440, 2808, 2812, 2875, 2880, 2913, 2916
$(CH_3)_2CClO_2$:	241, 295, 334, 370, 433, 447, 662, 792, 914, 965, 991, 1119, 1148, 1188, 1190, 1378, 1391, 1428, 1434, 1444, 1452, 2859, 2863, 2929, 2935, 2939, 2941

Rotational Constants (cm^{-1}), Symmetry Numbers, and Rotational Barriers ($kJ\ mol^{-1}$)

Overall Rotations

CH_3CCl_2:[15]	$B = 0.1214$;	$\sigma = 1$
$CH_3CCl_2O_2$:	$B = 0.07165$;	$\sigma = 1$
$(CH_3)_2CCl$:	$B = 0.1641$;	$\sigma = 1$
$(CH_3)_2CClO_2$:	$B = 0.08812$;	$\sigma = 1$

Internal Rotations

CH_3CCl_2:[15]	$a_1(CH_3-CCl_2) = 5.492$;	$\sigma = 3$; $V_0 = 9.790$
$CH_3CCl_2O_2$:	$a_1(CH_3-CCl_2O_2) = 5.4165$;	$\sigma = 3$; $V_0 = 19.83$
	$a_2(CH_3CCl_2-O_2) = 1.1667$;	$\sigma = 1$; $V_0 = 13.09$
$(CH_3)_2CCl$:	$a_{1,2}(CH_3-CClCH_3) = 5.5903$;	$\sigma = 3$; $V_0 = 7.1844$
$(CH_3)_2CClO_2$:	$a_{1,2}(CH_3-C(CH_3)ClO_2) = 5.4512$;	$\sigma = 3$; $V_0 = 19.2031$
	$a_3((CH_3)_2CCl-O_2) = 1.42307$;	$\sigma = 1$; $V_0 = 11.2553$

Entropies Calculated Using the Above Models

$S°_{298}(CH_3CCl_2) = 314.7\ J\ mol^{-1}\ K^{-1}$ $S°_{298}(CH_3CCl_2O_2) = 360.2\ J\ mol^{-1}\ K^{-1}$

$S°_{298}((CH_3)_2CCl) = 321.3\ J\ mol^{-1}\ K^{-1}$ $S°_{298}((CH_3)_2CClO_2) = 361.0\ J\ mol^{-1}\ K^{-1}$

(periodic triple well) were approximated by a symmetrical ($\sigma = 3$) sinusoidal potential. Barrier heights for these degrees of freedom obtained at UHF/6-31G** and UMP2/6-31G** levels agree within 1 kJ mol^{-1} (UMP2-level values corrected for the zero-point vibrational energy were used in the models). The potential energy surfaces of the C−OO torsional motion in $CH_3CCl_2O_2$ and $(CH_3)_2CClO_2$ radicals have more complex shapes. For both radicals, the three torsional potential energy minima, calculated at the MP2 level, differ by only 0.5 kJ mol^{-1} (Table 5S). In each of the radicals, two of the three potential energy maxima were equal (corresponding to an O−O bond eclipsed with C−Cl bonds in $CH_3CCl_2O_2$, and C−C bonds in $(CH_3)_2CClO_2$). In the models of both radicals, C−OO torsions were treated as nonsymmetrical hindered rotations with symmetrical sinusoidal potential (triple well) with the barrier heights taken as an average of three maxima calculated at the UMP2/6-31G** level with corrections for the zero-point vibrational energy (scaled[19] by a factor of 0.91). Reduced moments of inertia for internal rotations were calculated from the structural data by method of Pitzer and Gwinn.[20,21] Thermodynamic functions of the hindered internal rotations were obtained from interpolation of the tables of Pitzer and Gwinn.[20] Vibrational frequencies obtained in ab initio calculations were scaled by a factor of 0.89.[19] Properties of the CH_3CCl_2, $CH_3CCl_2O_2$, $(CH_3)_2CCl$, and $(CH_3)_2CClO_2$ radicals used in thermodynamic calculations are listed in Table 5.

IV.2. Determination of $\Delta H°_{298}$ and $\Delta S°_{298}$ of the Reactions (1a,−1a) and (2a,−2a). The room-temperature enthalpies of reactions (1a,−1a) and (2a,−2a) were obtained from the data on $K_1(T)$ and $K_2(T)$ using a third-law analysis. First, the values of $\Delta G°_T$ of reactions (1a,−1a) and (2a,−2a) were obtained directly from the values of the equilibrium constant:

$$\ln(K_p/\mathrm{bar}^{-1}) = -\Delta G°_T/RT \qquad \text{(III)}$$

where K_p is the equilibrium constant in bar^{-1}.

The addition of a small "correction"

$$f(T) = \frac{\Delta H°_T - \Delta H°_{298}}{RT} - \frac{\Delta S°_T - \Delta S°_{298}}{R}$$

converts the right-hand-side of eq III to a linear function of $1/T$ with the intercept at $1/T = 0$ equal to $\Delta S°_{298}/R$ and slope of the function equal to $-\Delta H°_{298}/R$:

$$\ln(K_p) + f(T) = \frac{\Delta S°_{298}}{R} - \frac{\Delta H°_{298}}{RT}$$

The values of this "correction" function, $f(T)$ ($\leq 1\%$ of $\ln(K_p)$) were calculated using the models of CH_3CCl_2, $CH_3CCl_2O_2$, $(CH_3)_2CCl$, and $(CH_3)_2CClO_2$ radicals described above (Table 5). The resultant values of $f(T)$ are listed in Tables 3 and 4.

The values of $\Delta S°_{298}$ of reactions (1a,−1a) and (2a,−2a) were calculated using the above models of the involved species:

$$\Delta S°_{298} = -159.6 \pm 4.0\ \mathrm{J\ mol^{-1}\ K^{-1}}\ \text{for reaction 1a,−1a}$$

$$\Delta S°_{298} = -165.5 \pm 6.0\ \mathrm{J\ mol^{-1}\ K^{-1}}\ \text{for reaction 2a,−2a}$$

(uncertainties were estimated from the uncertainties in the parameters of the internal hindered rotors and low-frequency vibrations). The values of $\Delta H°_{298}$ were obtained from the slopes of the lines drawn through the experimental values of ($\ln(K_p) + f(T)$) and the calculated intercepts $\Delta S°_{298}/R$ (Figure 6):

$$\Delta H°_{298}\ (1a,-1a) = -112.2 \pm 2.2\ \mathrm{kJ\ mol^{-1}} \qquad \text{(IV)}$$

$$\Delta H°_{298}\ (2a,-2a) = -136.0 \pm 3.8\ \mathrm{kJ\ mol^{-1}} \qquad \text{(V)}$$

Error limits here are 2σ and include contributions resulting from the uncertainties in the entropies of reactions (1a,−1a) and (2a,−2a).

In principle, a second law analysis can be used to obtain both $\Delta H°_{298}$ and $\Delta S°_{298}$ of reactions (1a,−1a) and (2a,−2a) from the ($\ln(K_p) + f(T)$) vs $1/T$ dependence. However, considering the narrow temperature intervals of the experiments to determine $K_1(T)$ and $K_2(T)$ and the scattering of data due to experimental uncertainties, we prefer to use the third-law analysis based on the ab initio calculated values of entropy.

V. Discussion

This study provides the first experimental and theoretical investigation of the kinetics and thermochemistry of the reactions of CH_3CCl_2 and $(CH_3)_2CCl$ radicals with molecular oxygen.

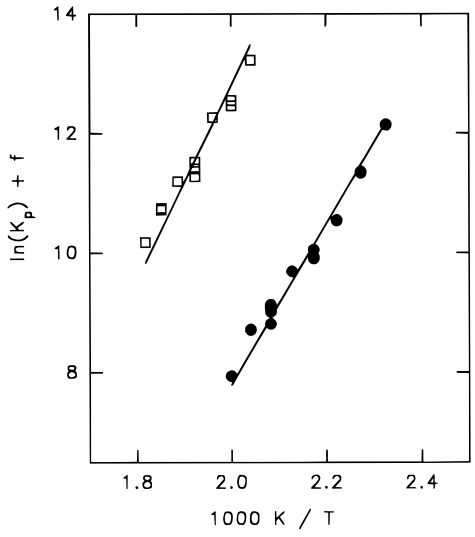

Figure 6. Modified van't Hoff plot of $(\ln(K_p) + f(T))$ vs 1000 K/T for reactions (1,−1) (circles) and (2,−2) (squares). Lines represent the results of the third-law fit (see text).

Similar systems studied experimentally before include the reactions of C_2H_5, CH_3CHCl, and i-C_3H_7 radicals with O_2. The reaction

$$C_2H_5 + O_2 \rightarrow \text{products} \qquad (8)$$

has received wide attention (refs 7 and 22−26 and references therein). The most widely discussed part of the mechanism of reaction 8 concerns the reaction pathway at high temperatures, where the equilibrium in the addition process $C_2H_5 + O_2 \rightleftarrows C_2H_5O_2$ is shifted to the left. While general agreement had been reached concerning the products of the high-temperature reaction ($C_2H_4 + HO_2$), uncertainty existed in the mechanism, i.e., whether these are the products of a direct abstraction reaction or a route involving the formation of an excited intermediate $C_2H_5O_2$ that undergoes further rearrangement leading to final products $C_2H_4 + HO_2$.

The most recent combined experimental and theoretical study[7] of reaction 8 decided in favor of the mechanism which proceeds through the formation of an excited adduct in the initial step of the reaction:

$$C_2H_5 + O_2 \underset{-8a}{\overset{8a}{\rightleftharpoons}} C_2H_5O_2 \xrightarrow{8b} CH_2CH_2OOH \rightarrow C_2H_4 + HO_2 \qquad (8)$$

This excited adduct can undergo decomposition back to reactants (−8a), stabilization, or rearrangement (8b) which finally leads to $C_2H_4 + HO_2$.

Such a mechanism quantitatively explains all the experimental data available on reaction 8, including the low-temperature kinetics (falloff in the bimolecular rate constant), equilibrium in the addition step (8a,−8a), high-temperature kinetics, and the product branching ratio as a function of temperature and pressure. The main argument that excludes the possible abstraction route is the absence of an apparent increase of the overall reaction rate constant with temperature at 750 K ≤ T ≤ 1002 K. Instead a slight decrease or independence of temperature of the overall rate constant was observed. Wagner et al.[7] suggested that the reaction pathway of excited $C_2H_5O_2$ leading to $C_2H_4 + HO_2$ proceeds via a five-member ring transition state to form CH_2CH_2OOH which subsequently decomposes. The rate-determining step is believed to be the hydrogen atom transfer. The barrier height for this hydrogen transfer proposed by Wagner et al. is 10 kJ mol^{-1} lower than the energy of reactants, $C_2H_5 + O_2$. Further support for this mechanism was given by the recent study of the pressure and temperature dependencies of the C_2H_4 yield in reaction 8 by Kaiser.[31]

In a later study[3] of the reaction of CH_3CHCl radicals with O_2, experimental data (low-temperature falloff behavior, equilibrium in the addition step at intermediate temperatures, and temperature-independent reaction at high temperatures) were interpreted in terms of an analogous mechanism:

$$CH_3CHCl + O_2 \underset{-9b}{\overset{9a}{\rightleftharpoons}} CH_3CHClO_2 \xrightarrow{9b} CH_2CHClOOH \rightarrow C_2H_3Cl + HO_2 \qquad (9)$$

The existence of a similar reaction mechanism was confirmed in the reaction of propyl radicals with O_2 by Kaiser and Wallington.[27] These authors experimentally determined the C_3H_6 yield in the room-temperature reaction of propyl radicals (mixture of i-C_3H_7 and n-C_3H_7 isomers) with molecular oxygen as a function of pressure in the interval 0.4−740 Torr. The C_3H_6 yield was inversely dependent on pressure, proving that it is formed via a rearrangement of an RO_2 adduct, a mechanism analogous to those of reactions 8 and 9.

A recent ab initio study of Ignatyev et al.[28] suggests an alternative mechanism of the $C_2H_5O_2$ rearrangement proceeding without the formation of the CH_2CH_2OOH intermediate but rather via a direct concerted olefin elimination:

$$C_2H_5 + O_2 \underset{-8a}{\overset{8a}{\rightleftharpoons}} C_2H_5O_2 \xrightarrow{8c} C_2H_4 + HO_2 \qquad (8')$$

These authors concluded that the energy barrier for the reaction step 8c is lower than that for 8b and is below the energy of $C_2H_5 + O_2$ reactants. Similar mechanisms of further RO_2 rearrangement can be present in other $R + O_2$ reactions. The observed kinetic behavior of reactions 8 and 9 (as well as reactions of propyl radicals with O_2) can still be explained by modified mechanisms such as 8′ since the RO_2 rearrangement (8b or 8c) will remain the rate-determining step.

The qualitative kinetic behavior of reactions 1 and 2, those of CH_3CCl_2 and $(CH_3)_2CCl$ with molecular oxygen, is very similar to that of reactions 8 and 9 at low (falloff in the room-temperature rate constants) and at intermediate temperatures (equilibrium in the $R + O_2 \rightleftarrows RO_2$ step). In the high-temperature regions, however, the analogy is incomplete. While the rate constant of reaction 2 is independent of temperature at T = 600−700 K (suggesting a mechanism similar to reactions 8 and 9), that of reaction 1 increases with temperature with an activation energy of 50.8 kJ mol^{-1} and a preexponential factor of 1.7×10^{-12} cm^3 molecule^{-1} s^{-1} (formula I). Such kinetic behavior of reaction 1 can be explained both by a mechanism similar to reactions 8 and 9:

$$CH_3CCl_2 + O_2 \underset{-1a}{\overset{1a}{\rightleftharpoons}} CH_3CCl_2O_2 \xrightarrow{1b} (CH_2CCl_2{-}OOH\rightarrow)\, HO_2 + CH_2{=}CCl_2 \qquad (A)$$

(with the potential energy barrier height for step 1b higher than the energy of reactants, $CH_3CCl_2 + O_2$), and by a direct abstraction reaction:

$$CH_3CCl_2 + O_2 \rightarrow HO_2 + CH_2{=}CCl_2 \qquad (B)$$

Unfortunately, the current experimental kinetic information on reaction 1 does not provide a basis for distinguishing between routes (A) and (B), thus leaving the question of the high-temperature mechanism open.

The results of the current study confirm the general trend of the weakening of the $R-O_2$ bond with the substitution of chlorine for hydrogen atoms on the carbon atom forming the C−O bond. This effect has been characterized for the case of $R = CH_3$. The bond strength ($DH°_{298}$) decreased[4−6,8] from 137 kJ mol^{-1} in CH_3-O_2 to 92 kJ mol^{-1} in CCl_3-O_2 with intermediate values of 122 kJ mol^{-1} for CH_2Cl-O_2 and 108 kJ mol^{-1} for $CHCl_2-O_2$. This phenomenon is consistent with the general weakening of the CH_3-X bond caused by the substitution of chlorine for hydrogen on the methyl group.[29] For $R = C_2H_5$, the presence of one Cl atom reduces the $R-O_2$ bond energy by 17 kJ mol^{-1} from 148 kJ mol^{-1} (in the case of $C_2H_5-O_2$)[6,7] to 131 kJ mol^{-1}.[3] As can be seen from the results of the current study, the presence of another Cl atom further reduces the $R-O_2$ bond strength (to 112.2 kJ mol^{-1}). An analogous effect is observed in the case of $R = i\text{-}C_3H_7$: the RO_2 bond energy is reduced from 155 kJ mol^{-1} in $(CH_3)_2CH-O_2$[6,14] to 136.0 kJ mol^{-1} in $(CH_3)_2CCl-O_2$.

Heats of formation of RO_2 radicals can be determined from the enthalpies of the $R + O_2 \rightleftarrows RO_2$ reactions and the heats of formation of R radicals. While $\Delta H_f°_{298}((CH_3)_2CCl)$ has not been experimentally determined, recommendations for $\Delta H_f°_{298}(CH_3CCl_2)$ have been published.[15,16] Chen and Tschuikow-Roux[15] obtained the value of $\Delta H_f°_{298}(CH_3CCl_2) = 51.0 \pm 5.9$ kJ mol^{-1} from competitive bromination studies of ethane and CH_3CHCl_2 by assuming equal activation energies for the reactions of CH_3CCl_2 and C_2H_5 with HBr. However, the difference between these activation energies has been experimentally determined to be 9.6 kJ mol^{-1} by Seetula,[16] who combined his data on the $CH_3CCl_2 + HBr$ reaction with those of Dymov and Tschuikow-Roux[17] on the reverse reaction ($Br + CH_3CHCl_2$) to obtain $\Delta H_f°_{298}(CH_3CCl_2) = 42.5 \pm 1.7$ kJ mol^{-1} in a second-law analysis. The credibility of this result is somewhat undermined by the unrealistic value of the CH_3CCl_2 entropy obtained in the second-law analysis ($S°_{298}(CH_3CCl_2) = 288 \pm 5$ J mol^{-1} K^{-1}, see section IV.1). If a more realistic $S°_{298}(CH_3CCl_2) = 314.7$ J mol^{-1} K^{-1} based on the ab initio calculations of Chen and Tschuikow-Roux[15] is used in a third-law analysis, it yields $\Delta H_f°_{298}(CH_3CCl_2) = 54.3$ kJ mol^{-1}, a value which, according to Seetula, is unrealistic since it implies equal α-C−H bond energies in 1,1-dichloroethane and dichloromethane.[16] A "theoretical" value $\Delta H_f°_{298}(CH_3CCl_2) = 49.2$ kJ mol^{-1} (calculated by Chen and Tschuikow-Roux[15] by coupling ab initio calculated energy changes for homodesmic reactions with the known heats of formation of other reaction components) is between the two extreme values obtained by Seetula in the second-law (42.5 ± 1.7 kJ mol^{-1}) and the third-law (54.3 kJ mol^{-1}) analyses. Considering the above factors contributing to the uncertainty of the CH_3CCl_2 thermochemistry, we choose for further use the average value of $\Delta H_f°_{298}(CH_3CCl_2) = 48.4 \pm 7.6$ kJ mol^{-1}, the error limits of which encompass both the second-law and the third-law values of Seetula. Combining this value with $\Delta H°_{298}(1a,-1a) = -112.2 \pm 2.2$ kJ mol^{-1} (expression (IV)), we obtain $\Delta H_f°_{298}(CH_3CHClO_2) = -63.8 \pm 9.8$ kJ mol^{-1}.

VI. Summary

The kinetics of the reactions

$$CH_3CCl_2 + O_2 \underset{-1a}{\overset{1a}{\rightleftharpoons}} CH_3CCl_2O_2 \rightarrow \text{products} \qquad (1)$$

$$(CH_3)_2CCl + O_2 \underset{-2a}{\overset{2a}{\rightleftharpoons}} (CH_3)_2CClO_2 \rightarrow \text{products} \qquad (2)$$

have been studied over wide ranges of temperatures and pressures. Distinctly different kinetic behavior at low (room temperature), high (791−1000 K, reaction 1; 600−700 K, reaction 2), and intermediate (430−500 K, reaction 1; 490−550 K, reaction 2) temperatures was investigated.

Equilibrium constants of reaction (1a,−1a) and (2a,−2a) were determined as functions of temperature. Structure and vibrational frequencies of $(CH_3)_2CCl$, $CH_3CCl_2O_2$, and $(CH_3)_2CClO_2$ were calculated by ab initio methods. The results were used to calculate the entropy changes of reactions (1a,−1a) and (2a,−2a) and, in combination with the experimental equilibrium data, to obtain the $R-O_2$ bond energies for reactions 1 and 2.

Acknowledgment. This research was supported by the National Science Foundation, Division of Chemical, Biochemical and Thermal Engineering under Grant CTS-9311848.

Supporting Information Available: Tables 1S−5S containing information on the properties of $CH_3CCl_2O_2$, $(CH_3)_2CCl$, and $(CH_3)_2CClO_2$ radicals determined in the ab initio study and Figures 1S−4S presenting the k' vs $[O_2]$ dependencies obtained in the room temperature and high-temperature experiments (16 pages). Ordering information is given on any current masthead page.

References and Notes

(1) Fenter, F. F.; Lightfoot, P. D.; Caralp, F.; Lesclaux, R.; Niiranen, J. T.; Gutman, D. *J. Phys. Chem.* **1993**, *97*, 4695.

(2) Fenter, F. F.; Lightfoot, P. D.; Niiranen, J. T.; Gutman, D. *J. Phys. Chem.* **1993**, *97*, 5313.

(3) Knyazev, V. D.; Bencsura, A.; Dubinsky, I. A.; Gutman, D.; Melius, C. F.; Senkan, S. M. *J. Phys. Chem.* **1995**, *99*, 230.

(4) Russell, J. J.; Seetula, J. A.; Gutman, D.; Danis, F.; Caralp, F.; Lightfoot, P. D.; Lesclaux, R.; Melius, C. F.; Senkan, S. M. *J. Phys. Chem.* **1990**, *94*, 3277.

(5) Russell, J. J.; Seetula, J. A.; Gutman, D.; Melius, C. F.; Senkan, S. M. *Symp. (Int.) Combust., Proc.* **1990**, *23*, 163.

(6) The values of $DH°_{298}(R-O_2)$ were obtained earlier using the experimentally determined temperature dependencies of the equilibrium constants of the corresponding $R + O_2 \rightleftarrows RO_2$ reactions. In all but one of these studies,[3] the interpretation of the experimental double-exponential kinetics (similar to that described in section 3.3) did not account for a possibility of further reaction (rearrangement or wall reaction) of the RO_2 adduct. Our reinterpretation of the experimental data of these earlier studies results in changes to the $DH°_{298}(R-O_2)$ values (Knyazev, V. D.; Slagle, I. R. *J. Phys. Chem. A* **1998**, *102*, 1770) which are reflected in the values cited in the current article.

(7) Wagner, A. F.; Slagle, I. R.; Sarzynski, D.; Gutman, D. *J. Phys. Chem.* **1990**, *94*, 1853.

(8) Slagle, I. R.; Gutman, D. *J. Am. Chem. Soc.* **1985**, *107*, 5342.

(9) Krasnoperov, L. N.; Niiranen, J. T.; Gutman, D.; Melius, C. F.; Allendorf, M. D. *J. Phys. Chem.* **1995**, *99*, 14347.

(10) Slagle, I. R.; Ratajczak, E.; Gutman, D. *J. Phys. Chem.* **1986**, *90*, 402.

(11) Slagle, I. R.; Park, J.-Y.; Gutman, D. *Symp. (Int.) Combust. [Proc.]* **1984**, *20*, 733.

(12) Okabe, H. *Photochemistry of small molecules*; Wiley: New York, 1978.

(13) Bevington, P. R. *Data Reduction and Error Analysis for the Physical Sciences*; McGraw-Hill: New York, 1969.

(14) Slagle, I. R.; Ratajczak, E.; Heaven, M. C.; Gutman, D.; Wagner, A. F. *J. Am. Chem. Soc.* **1985**, *107*, 1838.

(15) Chen, Y.; Tschuikow-Roux, E. *J. Phys. Chem.* **1992**, *96*, 7266.

(16) Seetula, J. A. *J. Chem. Soc., Faraday Trans.* **1996**, *92*, 3069.

(17) Dymov, B. P.; Tschuikow-Roux, E, conference abstract presented at the Pacific Rim Conference in Honolulu, Hawaii, Dec 1995.

(18) Gaussian 92, Revision E.1; Frisch, M. J.; Trucks, G. W.; Head-Gordon, M.; Gill, P. M. W.; Wong, M. W.; Foresman, J. B.; Johnson, B. G.; Schlegel, H. B.; Robb, M. A.; Replogle, E. S.; Gomperts, R.; Andres, J. L.; Raghavachari, K.; Binkley, J. S.; Gonzalez, C.; Martin, R. L.; Fox, D. J.; Defrees, D. J.; Baker, J.; Stewart, J. J. P.; Pople, J. A. Gaussian, Inc.: Pittsburgh, PA, 1992.

(19) Pople, J. A.; Scott, A. P.; Wong, M. W.; Radom, L. *Isr. J. Chem.* **1993**, *33*, 345.

(20) Pitzer, K. S.; Gwinn, W. D. *J. Chem. Phys.* **1942**, *10*, 428.

(21) Pitzer, K. S. *J. Chem. Phys.* **1946**, *14*, 239.

(22) Slagle, I. R.; Feng, Q.; Gutman, D. *J. Phys. Chem.* **1984**, *88*, 3648.

(23) Kaiser, E. W.; Lorkovic, I. M.; Wallington, T. J. *J. Phys. Chem.* **1990**, *94*, 3352.
(24) Bozzelli, J. W.; Dean, A. M. *J. Phys. Chem.* **1990**, *94*, 3313.
(25) Quelch, G. E.; Gallo, M. M.; Schaefer H. F., III *J. Am. Chem. Soc.* **1992**, *114*, 8239.
(26) Quelch, G. E.; Gallo, M. M.; Shen, M. Z.; Xie, Y. M.; Schaefer, H. F., III.; Moncrieff, D. *J. Am. Chem. Soc.* **1994**, *116*, 4953.
(27) Kaiser, E. W.; Wallington, T. J. *J. Phys. Chem.* **1996**, *100*, 18770.
(28) Ignatyev, I. S.; Xie, Y.; Allen, W. D.; Schaefer, H. F., III *J. Chem. Phys.* **1997**, *107*, 141.
(29) Weissman, M.; Benson, S. W. *J. Phys. Chem.* **1983**, *87*, 243.
(30) Tschuikow-Roux, E.; Niedzielski, J.; Faraji, F. *Can. J. Chem.* **1985**, *63*, 1093.
(31) Kaiser, E. W. *J. Phys. Chem.* **1995**, *99*, 707.